

Assessing Land Use/Land Cover Change Using Multitemporal Landsat Data in Agadir City (Morocco)



Ijjou Idoumskine, Ali Aydda, Abdelkrim Ezaidi, and Omar F. Althuwaynee

Abstract The aim of this study is to highlight Land Use/Land Cover (LULC) sever changes dynamics in Agadir city of Morocco during the period 1986–2019. For this purpose, Landsat imageries (5 TM, 7 ETM+, and 8 OLI) acquired in 1986, 1996, 2003, 2014, and 2019 years, were classified using Support Vector Machine (SVM) algorithm to produce LULC maps. First, spectral indices such as the Normalized Difference Vegetation Index (NDVI) and the Normalized Difference Built-up (NDBI) were used to discriminate the four LULC classes (built-up areas, bare lands, vegetation, and water bodies) of the study area. Moreover, change detection was applied on classified maps to characterize LULC dynamics class by class. The results reveal a spatial expansion over the 33 years, with high overall accuracy and kappa coefficient values. In detail, vegetation and bare lands have been decreased by 95.58% and 72.06%, respectively, while the built-up areas have been increased by an amount of 66.86%. Overall, the findings of this study could assist planners and decision-makers to guide, in a good manner, the sustainable land development of the city.

Keywords NDVI · NDBI · Supervised classification · Change detection · Landsat imagery

1 Introduction

It was recognized that Land Use/Land Cover (LULC) changes lead to severe environmental problems (climate change, ecosystem degradation, etc.). In light of this fact, whatever the causing act (natural or anthropic), it is essential to assess

I. Idoumskine (✉) · A. Aydda · A. Ezaidi
Department of Geology, Faculty of Sciences, Ibn Zohr University, Agadir, Morocco

O. F. Althuwaynee
Department of Energy and Mineral Resources Engineering, Sejong University, Seoul, Republic of Korea

and analyze LULC changes to understand its processes and to ensure a sustainable management (guide urbanization expansion, conserve ecosystem, etc.).

Practically, several studies have shown the strength of remote sensing and Geographical Information System (GIS) techniques for mapping production, detecting, and analyzing LULC changes and its environmental impacts [1–3]. Xiuwan [1] used multi-temporal Landsat TM to map and analyze land cover (LC) changes in the west coastal zone of Korea (Ansan City). Fichera et al. [2] used aerial photos and multitemporal Landsat TM scenes to map and analyze LC changes in the area of Avellino (south of Italy). Ahmed and Akter [3] used Landsat multi-spectral surface reflectance data to detect LC changes in southwest Bengal delta (Bangladesh). Bouiadjra et al. [4] used two scenes of Landsat imagery to assess vegetation cover change in Tessala mountains (Algeria).

Object-based classification is the most commonly used method to map LULC, and post-classification change detection technique is the most one used for analyzing surface change. Moreover, spectral indices of Normalized Difference Vegetative Index (NDVI), Normalized Difference Water Index (NDWI), and Normalized Difference Built-up Index (NDBI) are widely used to extract LULC.

In Morocco, where the overexploitation of natural resources associated with intense urbanization is prevailing, the rates of LULC dynamics are changing fast over the last decade. El Garouani et al. [5] used two Landsat (TM and ETM+) scenes to map land cover change and soil erosion within the Oued Tlata basin (northeast of Morocco). Mohajane et al. [6] trait the issue of vegetation changes in the Azrou Forest, Middle Atlas of Morocco, between 1987 and 2017 and the effects of LULC change on land surface temperature using multi-temporal Landsat satellite imagery. These studies and others have authenticated the LULC conversion throughout the kingdom.

In Agadir city, one of the largest seaside resorts in Morocco, as the process of urbanization becomes more intense in parallel with the start of the socio-economic development and the globalization of the city, the demand of land for various urban activities increases (in particular for secondary and tertiary activities). Hence, it is important to evaluate the magnitude and spatial extent of these changes within the city to ensure best future planning and management of land.

The present study anticipated to integrate NDVI and NDBI with object-based classification and post-classification change detection method in order to assess the spatiotemporal LULC changes in Agadir city during the period between 1986 and 2019.

2 Materials and Method

2.1 Study Area

Agadir city is the capital of Souss-Massa region and one of 13 administrative districts, which occupies the southern Moroccan Atlantic coast, with an approximate area of 112 km² [7] (Fig. 1).

Demographically, the district of Agadir had the highest growth rate in Morocco recorded at 3.7% during the period 1982–1994 [7]; the rural exodus was one of the main reasons for the population growth. Currently, the city experienced again an exceptional population growth, of about 421,844 inhabitants, according to the 2014 census [7]. The economy of the city prevails by tertiary activities (more than 50% of the territory), industry, trade, and fishery.

Geographically, Agadir city is marked by a semiarid climate with 340 sunshine days per year. The average annual temperature ranges from 14 °C to 16 °C in January and 19 °C to 25 °C in July. August is the hottest month (average temperature equal to 22.6 °C), while January is the coldest month (average temperature is 13.9 °C) and the annual precipitation is about 250 mm [8].

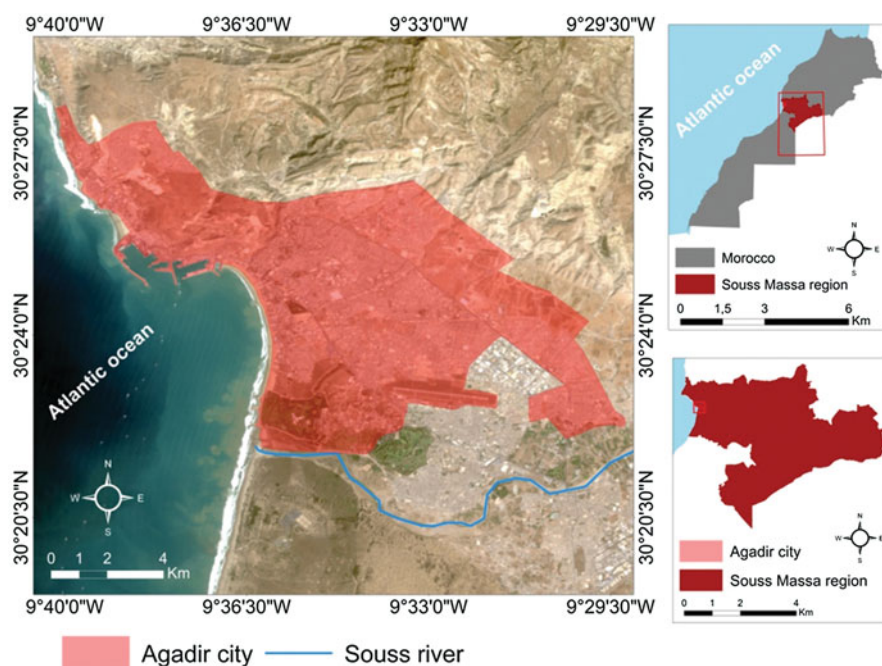


Fig. 1 Location map of the study area

Table 1 Characterizations of the used Landsat data

Acquisition dates	Satellite (sensor)	Bands number	Wavelength (μm)	Spatial resolution (m)
11/02/1986 07/02/1996	Landsat 5 (TM)	Band 1 blue	0.45–0.52	30
		Band 2 green	0.52–0.60	30
		Band 3 red	0.63–0.69	30
		Band 4 NIR	0.76–0.90	30
		Band 5 SWIR1	1.55–1.75	30
		Band 6 thermal	10.40–12.50	120
		Band 7 SWIR2	2.08–2.35	30
11/02/2003	Landsat 7 (ETM+)	Band 1 blue	0.45–0.52	30
		Band 2 green	0.52–0.60	30
		Band 3 red	0.63–0.69	30
		Band 4 NIR	0.77–0.90	30
		Band 5 SWIR1	1.55–1.75	30
		Band 6 thermal	10.40–12.50	60
		Band 7 SWIR2	2.09–2.35	30
		Band 8 pan	0.52–0.90	15
08/02/2014 22/02/2019	Landsat 8 (OLI)	Band 1 coastal	0.43–0.45	30
		Band 2 blue	0.45–0.51	30
		Band 3 green	0.53–0.59	30
		Band 4 red	0.63–0.67	30
		Band 5 NIR	0.85–0.88	30
		Band 6 SWIR1	1.57–1.65	30
		Band 7 SWIR2	2.11–2.29	30
		Band 8 pan	0.50–0.68	15
		Band 9 cirrus	1.36–1.38	30

2.2 Dataset

Satellite Data In this study, remote sensing imagery data were used from Landsat 5 Thematic Mapper (TM), Landsat 7 Enhanced Thematic Mapper Plus (ETM+), and Landsat 8 Operational Land Imager (OLI). All data provided free of charge from the United States Geological Survey website (USGS) [9]. The dates of all images were chosen, in all, to be as closely as possible and in the same climate and vegetation season, and to achieve a homogeneous selection of acquisition dates and conditions of none or little cloudiness. Table 1 shows all information about the used Landsat imagery data.

Auxiliary Data Other geospatial data were used to represent the study area and to validate LULC classification maps. These data include ESRI shapefile administrative boundary of Agadir city, satellite images archive from Google Earth imagery and GP points collected during a field survey using Global Positioning System (GPS) receivers of Mobile Topographer 9.3.2 Apk for Android.

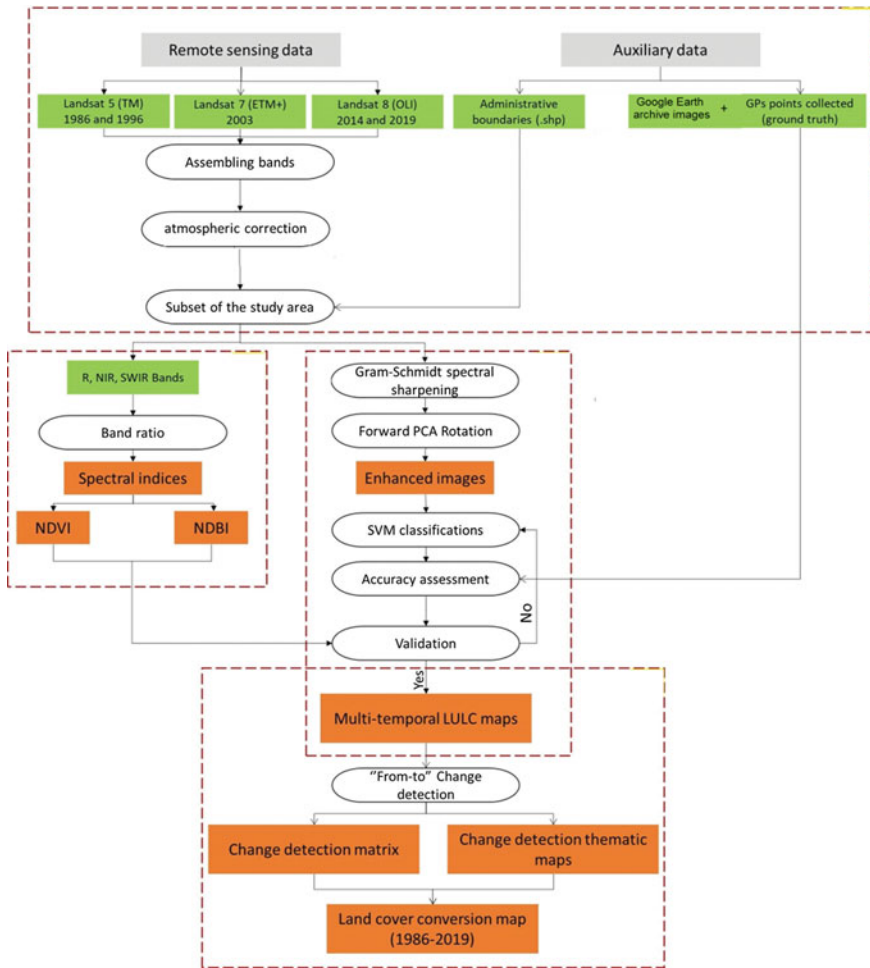


Fig. 2 Flowchart of the study

2.3 Methodology

The methodology followed in this study includes database preparation, indices extraction (NDVI and NDBI), classification and accuracy assessment, and change detection analysis. The flowchart used is summarized in Fig. 2.

Database Preparation All Landsat images used in this study were acquired in level 1T (LIT), which are already radiometrically calibrated and orthorectified [9].

First, the digital number (DN) value of each combined bands of each scene was converted to reflectance value by using ENVI 5.3 software. Then, the derived bands were atmospherically corrected by using Fast Line-of-sight Atmospheric Analysis

of Hypercubes (FLAASH) atmospheric correction model. Then, the corrected bands were clipped and subset to occupy the study area using the geo-referenced outline boundary of Agadir city.

Indices Extraction The use of index-based biophysical parameters to indicate relative abundance of features of interest are widely used in image processing. NDVI (Eq. 1) and NDBI (Eq. 2) were used for improving classification results and assisting land change detection task. However, these indices consist of spectral bands; the Red, Shortwave Infrared (SWIR) and the Near-Infrared (NIR) intervals of the electromagnetic spectrum.

$$\text{NDVI} = (\text{NIR} - \text{red}) / (\text{NIR} + \text{red}) \quad (1)$$

$$\text{NDBI} = (\text{SWIR} - \text{NIR}) / (\text{SWIR} + \text{NIR}) \quad (2)$$

Supervised Classification Implemented to classify the total of surface cover using training samples, collected from knowing points (representative classes) based on supervised machine learning. In this study, Support Vector Machine (SVM) algorithm used due to its ability to handle small training data sets [10] and often produces higher classification accuracy than the traditional methods [10, 11]. The representative LULC classes in our study area are built-up, vegetation, bare land, and water (Table 2).

Several spectral improvements were performed before starting supervised classification. Gram-Schmidt spectral sharpening was applied on prepared data of Landsat 7 ETM+ and Landsat 8 OLI in order to adjust their spatial resolution by using their own panchromatic band. Furthermore, for each scene, the principal component analysis (PCA) was applied to compress the redundant data of the used multibands and only the three first components which have maximum spectral information are used for classification.

Post-classification Change Detection All classified maps have been converted into polygon features (shapefile vector format) in order to evaluate and detect LULC change. The change detection was achieved by using vector spatial analysis (Intersect and Union) tools of ArcGIS 10.3 software.

Table 2 Land cover classes

LULC classes	Description
Urban	Residential, commercial, industrial, transportation, and facilities
Vegetation	Urban vegetation including parks and gardens
Bare land	Open spaces without vegetation or urban cover
Water	Rivers, lakes, or swimming pools

3 Results and Discussion

3.1 NDVI and NDBI Indices

Vegetation and built-up areas of each scene were extracted by using NDVI and NDBI indices (Fig. 3). Commonly, the NDVI values varies between -1 and 1 ; the values from -1 to 0 represent deep water, barren rocks, sand, or snow while the values between 0 and 1 indicate high to moderate density vegetation [12]. Moreover, the positive values of NDBI indicate built-up areas while negative values represent water bodies [13].

3.2 LULC Classification and Accuracy Assessment

LULC maps produced by SVM classifications were evaluated by using the error matrix, which consists of producer and user accuracies developed to compare randomly chosen test pixels with used ones for classification. For each scene, we have repeated the classification step many time until the best results of accuracy are obtained.

The final version of classified maps is shown in Fig. 4. Due to the heterogenic and the variability of urban cover of the study area; especially in its middle part, we could not obtain higher overall accuracies than the ones presented, even after repeating the classifications many times.

The kappa coefficients and overall accuracies achieved for final LULC maps are given in Table 3. Generally, the overall accuracy of all classified maps is higher than 80% , which means we have achieved the best classification for all used Landsat scenes.

3.3 LULC Change Detection

The statistical analysis of LULC change for the period 1986–2019 in Agadir city is shown in Figs. 5 and 6.

Effectively, during the 33 years, we remark an important growth of built-up class by 98.21% (24.78 km^2). Meanwhile, the bare land was reduced by 1.73 km^2 (6.84%) as compared to 8.11 km^2 (24.95%), 64.09 km^2 (26.68%), and 1.36 km^2 (4.75%) during the interval periods 1996–2003, 2003–2014, and 2014–2019, respectively, with a total amount of 26.84 km^2 (47.18%) for the entire period of the study. The vegetation cover had increased by 27.01 km^2 (422.85%) during the period 1986–1996, then had decreased by 7.98 km^2 (-23.95%), 10.06 km^2 (-39.56%), and 1.78 km^2 (-16.50%), respectively, during the interval periods 1996–2003, 2003–

2014, and 2014–2019. The water bodies have shown a relatively lower change rate during the period 1986–2019 (-0.89 km^2).

These results indicate that in 1986 as well as in 1996, the largest land cover class was bare land. After 2003, a strong growth of the urban land in line with population livelihood and economic activities (industrial and commercial) shows up and spread dramatically and affecting bare land and vegetation cover.

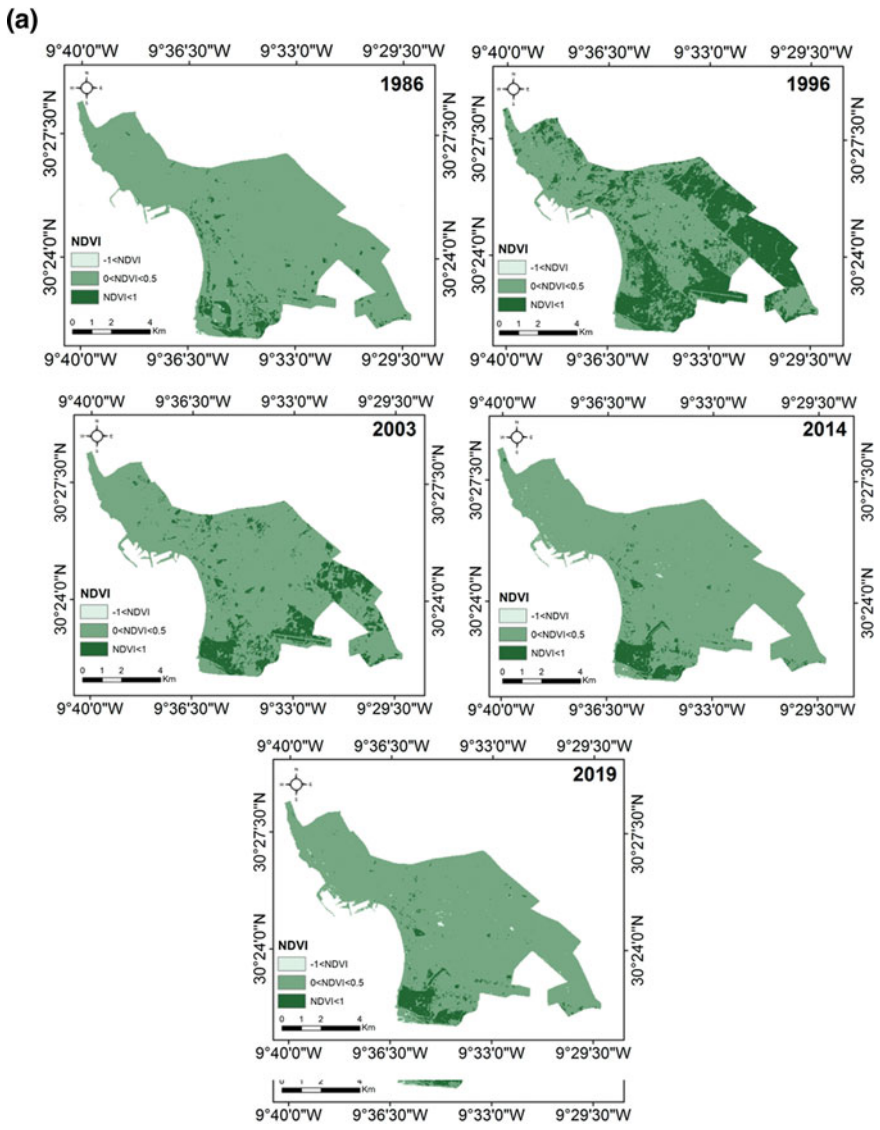


Fig. 3 Spatiotemporal distribution of NDVI (a) and NDBI (b)

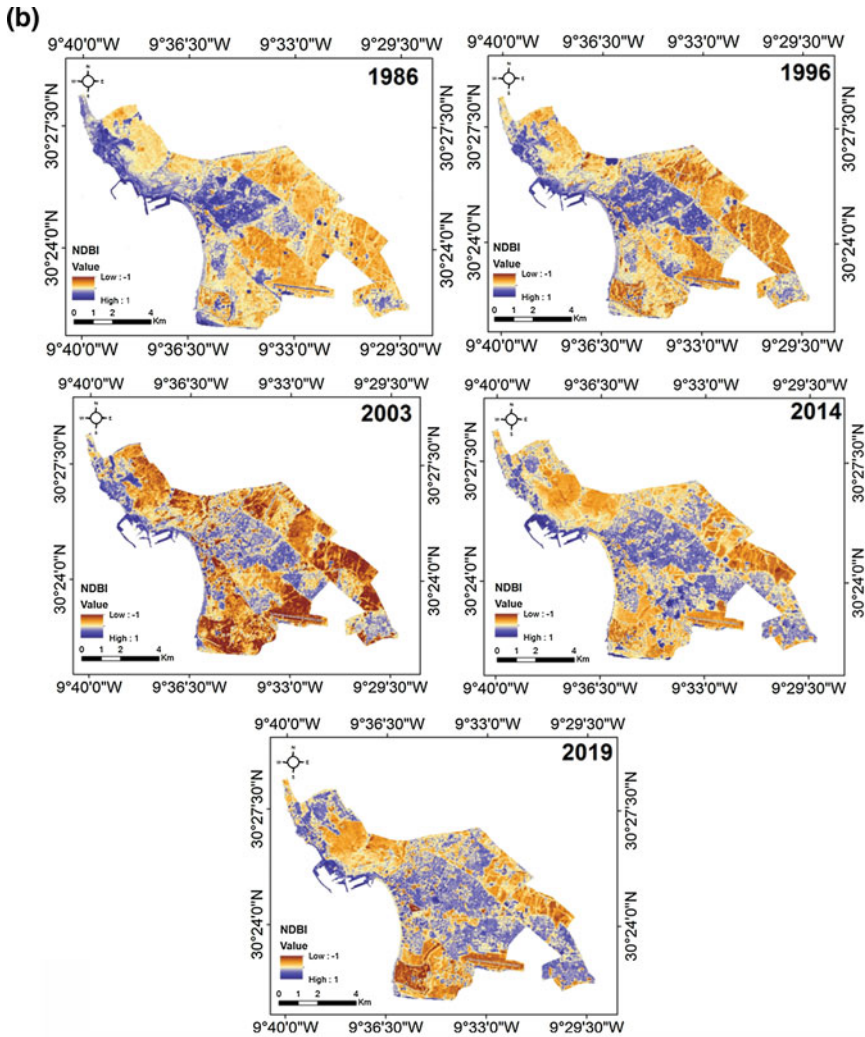


Fig. 3 (continued)

Consequently, we highlighted two clearly recognizable scenarios; (1) the urban area has increased drastically and rapidly, and (2) bare land and vegetation cover have gradually decreased.

Furthermore, LULC change map, for the interval period 1986–2019, indicates that the bare land was the main contributor in shaping urban area of the city followed by vegetation cover (Figs. 7 and 8).

Table 3 The accuracy assessment of classified LULC maps

LULC classes	Landsat 5 (TM)				Landsat 7 (ETM+)				Landsat 8 (OLI)					
	1986 classification		1996 classification		2003 classification		2014 classification		2019 classification		2019 classification		2019 classification	
	Producer (%)	User (%)	Producer (%)	User (%)	Producer (%)	User (%)	Producer (%)	User (%)	Producer (%)	User (%)	Producer (%)	User (%)	Producer (%)	User (%)
Bare land	73.42	97.31	97.85	94.79	96.41	99.77	32.62	97.80	65.79	98.78	65.79	97.80	65.79	98.78
Built-up	100.00	57.21	95.94	99.68	99.66	99.91	98.74	89.76	94.14	95.63	94.14	89.76	94.14	95.63
Vegetation	72.73	58.18	99.44	98.89	98.57	97.43	86.31	95.39	88.40	98.28	88.40	95.39	88.40	98.28
Water	100.00	98.94	0.00	0.00	100.00	99.77	11.11	20.00	37.50	21.82	37.50	20.00	37.50	21.82
Overall accuracy	85.45%		89.85%		98.97%		93.56%		81.83%		81.83%		81.83%	
Kappa	0.77		0.85		0.97		0.88		0.73		0.73		0.73	

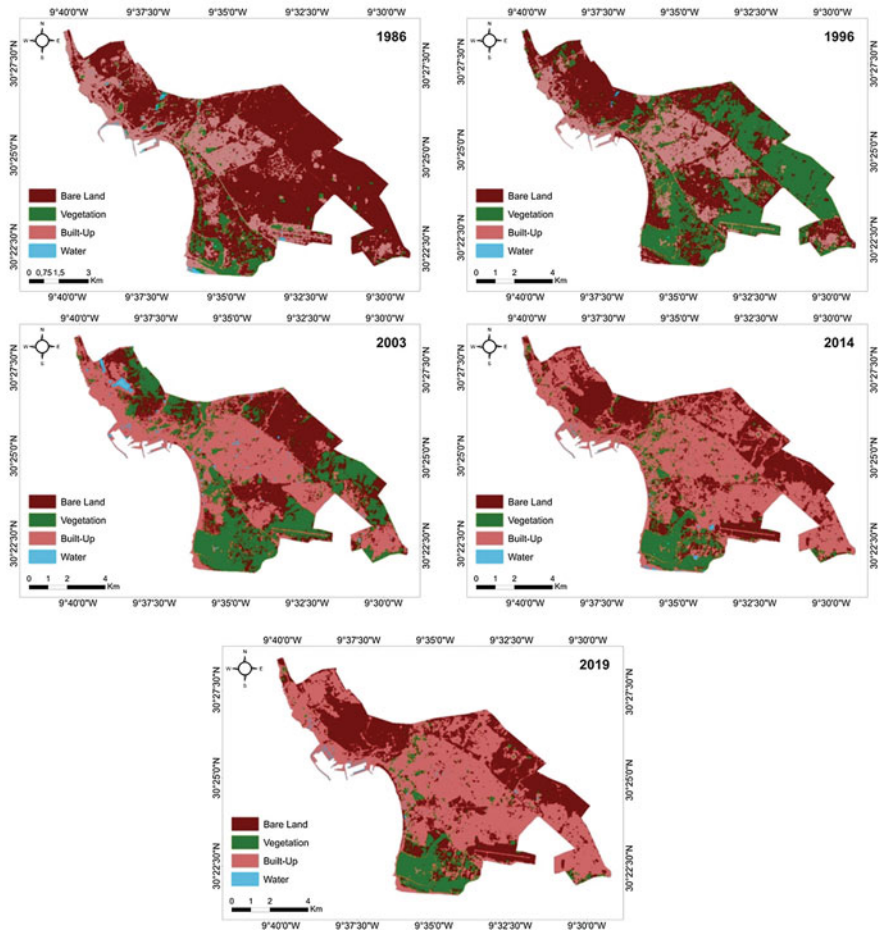


Fig. 4 LULC maps produced by classification process

Commonly, the LULC sever changes dynamics in Agadir city are caused by the urbanization activities and the construction of new urban areas in the early of 1960s after the 1960 earthquake. Moreover, the increase in area for urbanization purposes at the expense of vegetation and bare land, which have most suffered the effects of the expansion of the built-up areas, had many other reasons, such as the demographic crisis caused by the rural exodus of residents in surrounding rural areas and the economic development of the city during the last decades.

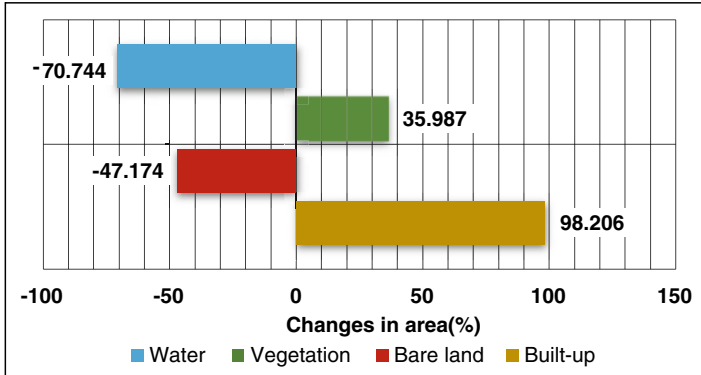


Fig. 5 LULC change area during the interval period 1986–2019

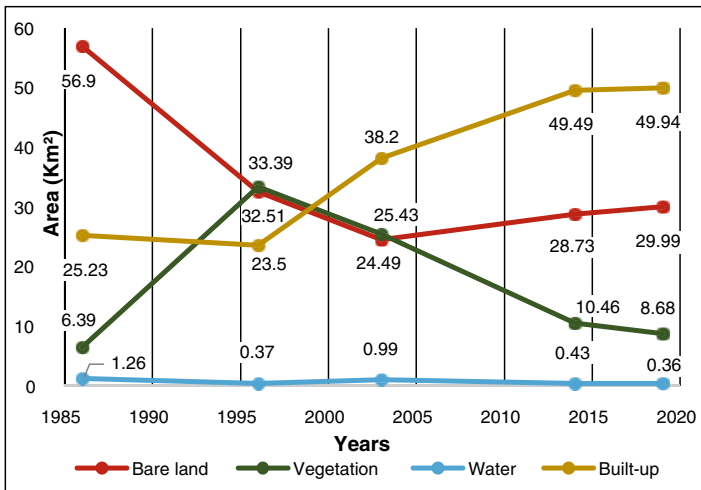


Fig. 6 LULC change scenario during the period 1986–2019

4 Conclusion

The multitemporal Landsat data, for Agadir city in Morocco for the period of 1986–2019, witnessed touchable variation in LULC spatial representation; therefore, it was processed to assess the change dynamics along that period. Several processing steps were conducted to achieve the main goal of the study, including spectral reflectance indices (NDVI and NDBI) extraction, SVM supervised classification, and post-classification comparison.

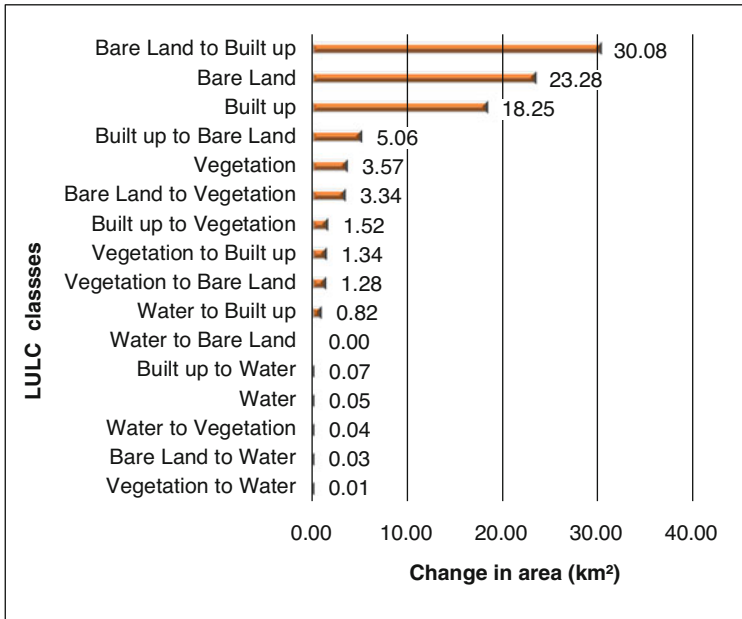


Fig. 7 Percentage of LULC classes conversion for the period 1986–2019

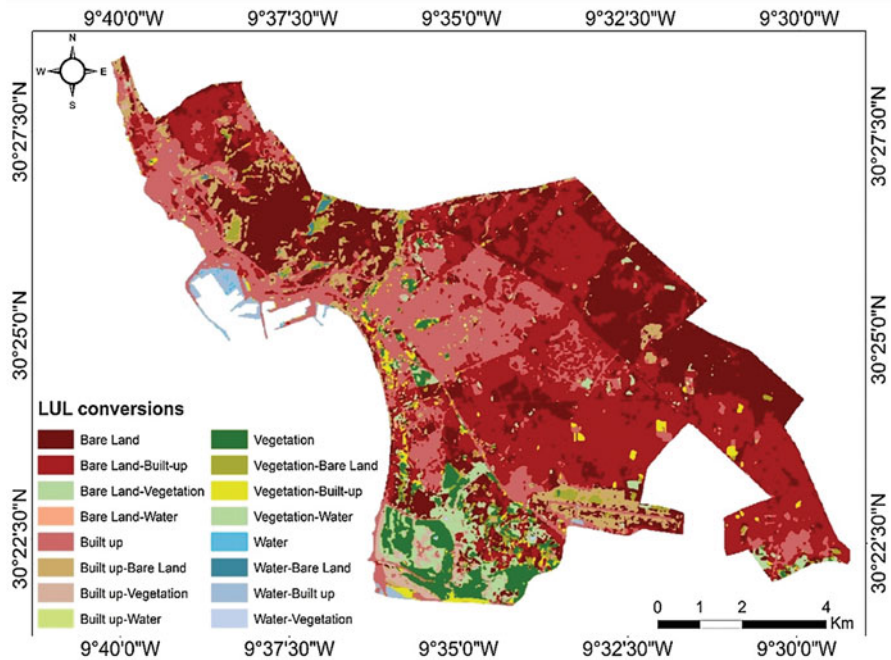


Fig. 8 Land cover conversion from 1986 to 2019

All the classified maps show a high statistical performance in terms of accuracy. The statistical results indicate an intense decreasing and rapidly changing trend in city over the last 33 years. It was found that the urban area has been increased, vegetative area and bare land have been decreased, and water bodies remained constant. The change detection map reveals that the bare land has been the main contributor in shaping urban area of the city followed by vegetation cover.

Eventually, after a successful application of the conducted study, where obtained results, can be an effective tool for land management and ecosystem conservation in the study area for next decade especially if were considered by city council and decision makers.

References

1. Xiuwan, C. (2002). Using remote sensing and GIS to analyse land cover change and its impacts on regional sustainable development. *International Journal of Remote Sensing*, 23(1), 107–124.
2. Fichera, C. R., Modica, G., & Pollino, M. (2012). Land cover classification and change-detection analysis using multi-temporal remote sensed imagery and landscape metrics. *European Journal of Remote Sensing*, 45(1), 1–18.
3. Ahmed, K. R., & Akter, S. (2017). Analysis of landcover change in Southwest Bengal delta due to floods by NDVI, NDWI and K-means cluster with Landsat multi-spectral surface reflectance satellite data. *Remote Sensing Applications: Society and Environment*, 8, 168–181.
4. Bouiadjra, S. E. B., Zerey, W. E., & Benabdeli, K. (2011). Étude diachronique des changements du couvert végétal dans un écosystème montagneux par télédétection spatiale: cas des monts du Tessala (Algérie occidentale). *Physio-Géo. Géographie Physique et Environnement*, 5, 211–225.
5. El Garouani, A., Chen, H., Lewis, L., Tribak, A., & Abharour, M. (2008). Cartographie de l'utilisation du sol et de l'érosion nette à partir d'images satellitaires et du sig idrisi au nord-est du Maroc. *Revue Télédétection*, 8(3), 193–201.
6. Mohajane, M., Essahlaoui, A., Oudija, F., El Hafyani, M., Hmaidi, A. E., El Ouali, A., Randazzo, G., & Teodoro, A. C. (2018). Land use/land cover (LULC) using landsat data series (MSS, TM, ETM+ and OLI) in Azrou Forest, in the Central Middle Atlas of Morocco. *Environments*, 5(12), 131.
7. HCP. *Recensement Général de la Population et de l'Habitat 2014 (RGPH)*. <https://rgph2014.hcp.ma>
8. *Climate charts Homepage*. <https://www.climate-charts.com/Locations/m/FM60250.html>
9. *USGS Homepage*. <https://www.usgs.gov/Landsat>
10. Mantero, P., Moser, G., Member, S., Serpico, S. B., & Member, S. (2005). Partially supervised classification of remote sensing images through SVM-based probability density estimation. *IEEE Transactions on Geoscience and Remote Sensing*, 43(3), 559–570.
11. Aydda, A., Althuwaynee, O. F., Algouti, A., & Algouti, A. (2019). Evolution of sand encroachment using supervised classification of Landsat data during the period 1987-2011 in a part of Laâyoune-Tarfaya basin of Morocco. *Geocarto International*, 34(13), 1514–1529.
12. Jackson, R. D., & Huete, A. R. (1991). Interpreting vegetation indices. *Preventive Veterinary Medicine*, 11(3–4), 185–200.
13. Zha, Y., Gao, J., & Ni, S. (2003). Use of normalized difference built-up index in automatically mapping urban areas from TM imagery. *International Journal of Remote Sensing*, 24(3), 583–594.